Eur Radiol (2007) 17: 509–522
DOI 10.1007/s00330-006-0180-y

Sungjun Kim
Jin-Young Choi
Yong-Min Huh
Ho-Taek Song
Sung-Ah Lee
Seung Min Kim
Jin-Suck Suh

Role of magnetic resonance imaging in entrapment and compressive neuropathy—what, where, and how to see the peripheral nerves on the musculoskeletal magnetic resonance image: part 2. Upper extremity

Received: 26 August 2005
Revised: 10 January 2006
Accepted: 26 January 2006
Published online: 30 March 2006

S. Kim · J.-Y. Choi · Y.-M. Huh · H.-T. Song · S.-A. Lee · J.-S. Suh (✉)
Department of Diagnostic Radiology,
College of Medicine,
Yonsei University,
134, Shinchondong, Seodaemun-ku,
120-752 Seoul, South Korea
e-mail: jss@yumc.yonsei.ac.kr
Tel.: +82-2-22287400
Fax: +82-2-3933035

S. Kim
Department of Diagnostic Radiology,
College of Medicine,
Hanyang University, Kuri Hospital,
Kuri City, Kyunggi-do 471-701,
South Korea

J.-S. Suh
Research Institute of Radiological
Science, College of Medicine,
Yonsei University,
134, Shinchondong, Seodaemun-ku,
120-752 Seoul, South Korea

S. M. Kim
Department of Neurology,
College of Medicine,
Yonsei University,
Seoul, South Korea

Abstract The diagnosis of nerve entrapment and compressive neuropathy has been traditionally based on the clinical and electrodiagnostic examinations. As a result of improvements in the magnetic resonance (MR) imaging modality, it plays not only a fundamental role in the detection of space-occupying lesions, but also a compensatory role in clinically and electrodiagnostically inconclusive cases. Although ultrasound has undergone further development in the past decades and shows high resolution capabilities, it has inherent limitations due to its operator dependency. We review the course of normal peripheral nerves, as well as various clinical demonstrations and pathological features of compressed and entrapped nerves in the upper extremities on MR imaging, according to the nerves involved. The common sites of nerve entrapment of the upper extremity are as follows: the brachial plexus of the thoracic outlet; axillary nerve of the quadrilateral space; radial nerve of the radial tunnel; ulnar nerve of the cubital tunnel and Guyon's canal; median nerve of the pronator syndrome, anterior interosseous nerve syndrome, and carpal tunnel syndrome. Although MR imaging can depict the peripheral nerves in the extremities effectively, radiologists should be familiar with nerve pathways, common sites of nerve compression, and common space-occupying lesions resulting in nerve compression in MR imaging.

Keywords Peripheral nerve · Anatomy · MR

Introduction

Nerve entrapment and compression syndrome (NECS) is the neurological symptom complex caused by the mechanical or dynamic compression of a segment of a single nerve at specific sites as it passes through a narrow fibro-osseous tunnel or an opening in a fibrous or muscular structure [1]. In general, the diagnosis of NECS has relied primarily upon clinical information, neurological examination, and electrodiagnostic studies. However, such clinical evaluations alone do not always allow one to arrive at a concrete diagnosis when the presentation is atypical and when anatomic and technical limitations for electrodiagnostic studies intervene. In these instances, imaging can play an important role in helping to define the site and etiology of nerve compression or in establishing an alternative diag-

nosis [2]. Hence, it has been widely reported that imaging modalities can feasibly demonstrate the causes and locations of NECS [1–11].

Ultrasound has undergone considerable development over the past decades. Although ultrasound shows higher resolution than any other current imaging modality, it remains limited in its ability to show pathological changes within nerves, owing to its poor soft tissue contrast compared with MR imaging. Moreover, the inherent operator dependency and the difficulty in fully covering the region of interest when evaluating deeper location have always been problems in ultrasound examination. As a current modality and because state-of-the-art MR imaging facilities show high performance in nerve imaging, MR imaging is a useful diagnostic tool for examining peripheral nerves. The ability of MR imaging to visualize the pathological characters of nerves and nerve-related lesions is superior to that of any other modalities.

Nerve entrapment and compression syndrome (NECS) of the upper extremity is more common and complex than that of the lower extremity. Although NECSs of the median nerve at the carpal tunnel and ulnar nerve at the cubital tunnel are the most common and familiar entities, there are various other entities that should be addressed.

In this article, we review the course of normal peripheral nerves in the upper extremity, as well as various clinical demonstrations and pathological features of compressed and entrapped nerves and innervated muscles in MR imaging, according to the nerves involved.

Brachial plexus

The brachial plexus is formed by the union of the ventral branches of the four lower cervical and first thoracic nerves. C5 and C6 nerve roots comprise the upper *trunk*, C7 continues to the middle *trunk*, and C8 and T1 comprise the lower *trunk*. The three trunks are formed within, or lateral to, the interscalene triangle, which is formed by the anterior scalene muscle, the middle and posterior scalene muscles, and the first rib. More laterally, the trunks divide into three anterior and three posterior *divisions*, and sub-

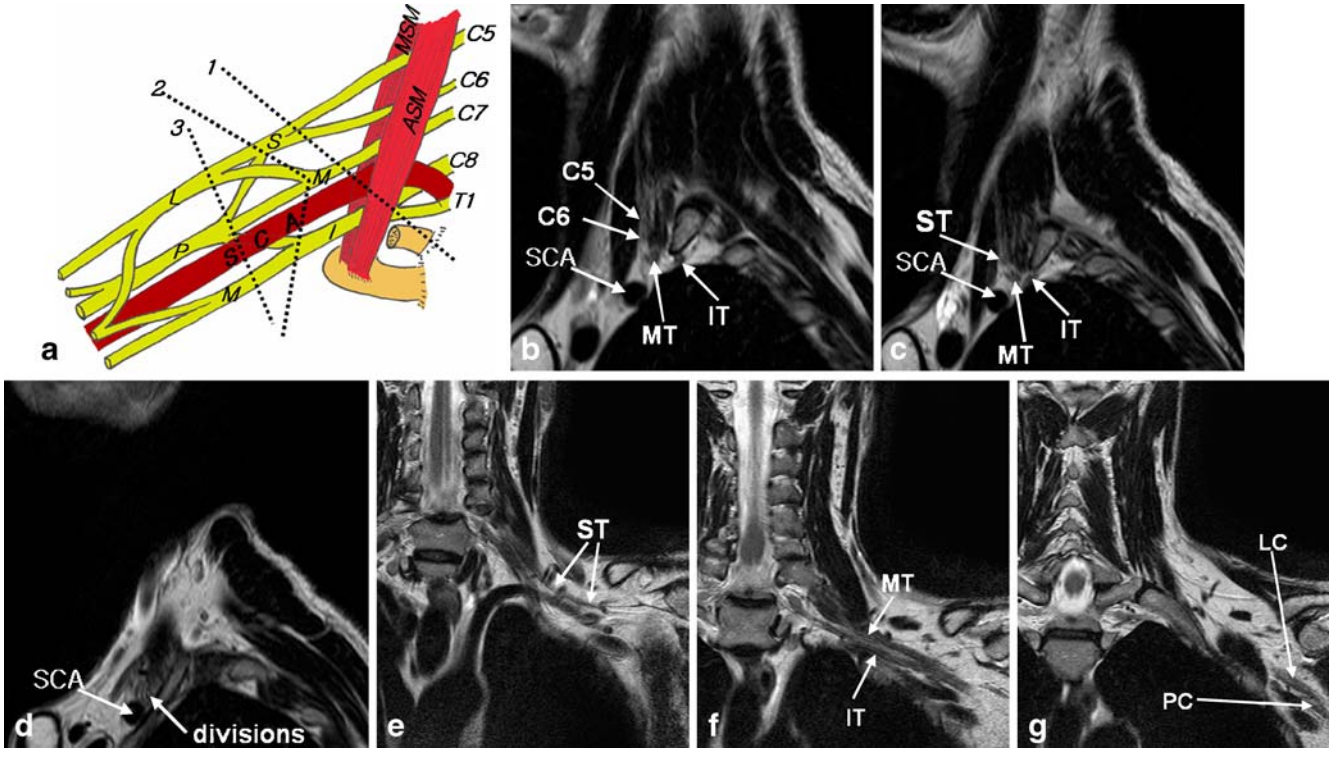

Fig. 1 Schematic diagram and MR imaging of the brachial plexus. **a** C5–T1 ventral rami comprise the brachial plexus. They pass between the anterior and middle scalene muscles (interscalene triangle) and form three trunks [superior trunk (*ST*), middle trunk (*MT*), and Inferior trunk (*IT*)] near the lateral margin of these muscles. The trunks split into three anterior and three posterior divisions more laterally at the superoposterior aspect of the subclavian artery (*SCA*). The plexus then merges into the lateral cord (*LC*), posterior cord (*PC*), and medial cord (*MC*), which subsequently form the nerves of the upper extremity. **b–d** Sagittal fast spin-echo T2-weighted images (FSE T2WIs) at the level proximal to *dotted line 1* (**b**), between 1 and 2 (**c**), and between 2 and 3 (**d**) labeled in **a**. Note the location of the subclavian artery and trunks of the brachial plexus within the interscalene triangle (**b**, **c**). The divisions of the brachial plexus are noted superoposterior to the subclavian artery as an intermediate signal dot (**d**). **e–g** Coronal FSE T2WIs at the plane between the anterior and middle scalene muscles (**e**, **f**) and at the plane of the costovertebral articulation (**g**). Note the locations of trunks and cords on the coronal images. *C5, C6* C5 and C6 ventral nerve roots

sequently join to form three *cords* distal to the lateral margin of the first rib. The cords end in five terminal branches of the median nerve, ulnar nerve, musculocutaneous nerve, axillary nerve, and radial nerve. The subclavian artery traverses the interscalene triangle along with the plexus. At the level of the axilla, the neurovascular complex within the axillary sheath consists of the axillary artery, the adjacent cords, and the axillary vein. The subclavian vein courses anterior to the anterior scalene muscle and does not pass through the interscalene triangle. The brachial plexus is well depicted on MR imaging on coronal and sagittal view through its course (Figs. 1 and 2).

Three typical syndromes, which are called the thoracic outlet syndrome (TOS), have been defined according to the zones that are prone to entrapment of the brachial plexus, subclavian artery, and subclavian veins. First, anterior scalene syndrome is a symptom complex that occurs when the brachial plexus and/or subclavian artery is compressed as it courses through the interscalene triangle. Second, costoclavicular syndrome is caused by the compression of one or several structures mentioned above between the clavicle and the first rib (costoclavicular space). Third, retropectoralis minor syndrome is caused by the compression of one or several structures mentioned above beneath the pectoralis minor at the site of attachment to the coracoid process, which is called the retropectoralis minor space (subcoracoid tunnel) [12–14].

The diagnosis of TOS is traditionally based on results of clinical evaluation, including various dynamic maneuvers such as elevation of the arm, because the symptom is better manifested with arm elevation. However, diagnosis based on clinical examination alone is often difficult. The contribution of MR imaging to the depiction of those three zones mentioned above has been researched by many investigators [14-17]. Thoracic outlet can be well visualized in MR imaging with the patient in a comfortable position with the arm alongside the body, but additional postural maneuver, including hyperabduction and external rotation of the arm, is needed in patients with TOS. Thoracic outlet was reported to be further narrowed, except in the interscalene triangle, with this additional postural maneuver, both in healthy volunteers and in the patients with TOS, and it was also reported that the patients with TOS had a significantly narrower costoclavicular space after the postural maneuver than did healthy volunteers [14].

Suprascapular nerve

The suprascapular nerve is a mixed motor and sensory nerve that carries pain fibers from the glenohumeral and acromioclavicular joints and provides motor supply to the supraspinatus and infraspinatus muscles. It arises from the superior trunk of the brachial plexus. The suprascapular nerve runs outwards, deep to the trapezius muscle and parallel to the omohyoid muscle, and enters the supraspinatus fossa through the suprascapular notch of the scapula. It winds around the lateral border of the spine of the scapula, passing the spinoglenoid notch to reach the infraspinatus fossa [18, 19]. A branch to the supraspinatus muscle forks off just after it traverses the suprascapular notch, and after it enters into the infraspinatus fossa, a branch to the infraspinatus divides off. Therefore, if a compressing lesion is around the scapular notch, then both the supraspinatus and the infraspinatus muscles are denervated. When a compressing lesion is located around the spinoglenoid notch, only the infraspinatus is denervated (Fig. 3) [20]. The etiologies of entrapment of the suprascapular nerve include fracture of the scapula, shoulder dislocation, tumor, compression by the suprascapular ligament during shoulder motion, depending on

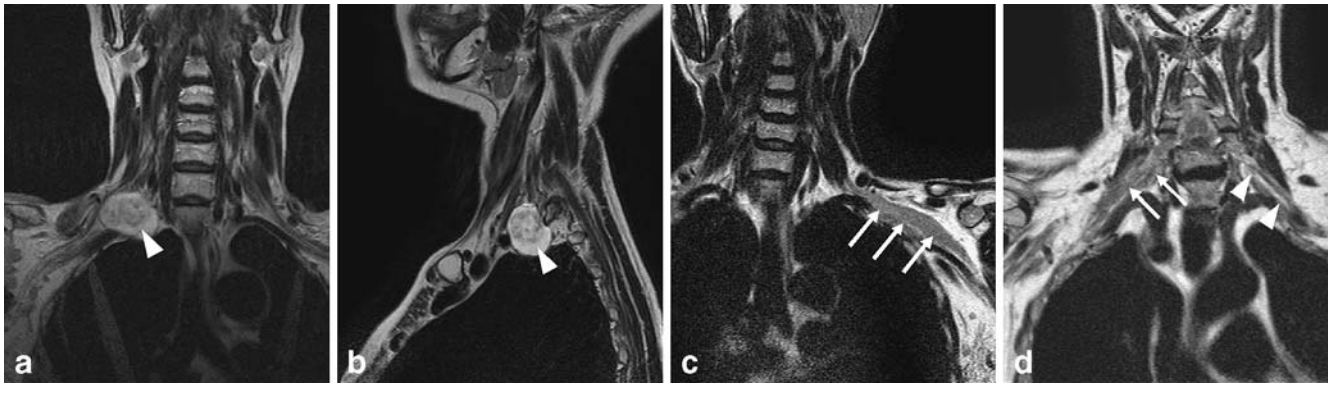

Fig. 2 Various MR imaging features of diseases involving the brachial plexus. **a**, **b** Schwannoma of brachial plexus depicted on MR imaging. Coronal (**a**) and sagittal (**b**) fast spin-echo T2-weighted images (FSE T2WIs) demonstrates a mass involving the inferior trunk of the right brachial plexus (*arrowheads*). **c** Inflammation of the brachial plexus depicted on MR imaging. Coronal FSE T2WI demonstrates diffuse thickening of the left brachial plexus (*arrows*). Diffuse inflammatory cell infiltration was confirmed on biopsy. **d** MR image obtained from a patient with lymphoma. Coronal FSE T2WI demonstrated thickening of the right brachial plexus. Please compare the normal left brachial plexus (*arrowheads*) with the abnormal right one (*arrows*). Biopsy was done for the right brachial plexus, and infiltration of lymphoma was confirmed

the shape of the suprascapular notch, and ganglion [18, 21, 22]. The ganglion is found more commonly near the spinoglenoid notch, and it is commonly associated with capsulolabral injury of the shoulder joint [19, 23]. Ganglia usually cause isolated denervation changes that affect the infraspinatus muscle, whereas a combined denervation change affecting both the supra- and infraspinatus muscles is more common in cases of nerve compression by the suprascapular ligament. Hence, a denervated muscle with signal changes indicates where the nerve is trapped or compressed [22] (Fig. 4). In cases of denervation signal changes of both the supra- and infraspinatus muscles without a definite lesion causing compression at the scapular notch, neuritis involving the suprascapular nerve (Parsonage–Turner syndrome) should be included in the differential diagnosis [24].

Axillary nerve (quadrilateral space syndrome)

The quadrilateral space is an anatomical compartment bordered by the subscapularis muscle anteriorly, teres minor muscle posteriorly, long head of the triceps muscle medially, and the surgical neck of the humerus laterally. The axillary nerve originates from the posterior cord of the brachial plexus (C6, C7), passes anterior to the subscapularis muscle, and then runs dorsally, together with the posterior circumflex humeral artery, through the quadrilateral space. The axillary nerve innervates the teres minor and deltoid muscles and has cutaneous sensory branches that extend to regions of the shoulder and upper arm.

Quadrilateral space syndrome is a rare entity in which the posterior humeral circumflex artery and the axillary nerve in the quadrilateral space are compressed by abduction and external rotation of the shoulder joint, causing poorly localized pain over the anterior aspect of the shoulder that may radiate to the arm and even to the forearm, with a non-dermatomal distribution [25]. Besides dynamic compression due to the position of the shoulder, the nerve can also be damaged or entrapped by static causes, such as fracture of the proximal humerus or scapula and associated hematoma, posteroinferior paralabral cysts, hypertrophy of the teres minor muscle, and fibrous bands [26–28]. The pathophysiology of quadrilateral space syndrome remains unclear. Some believe that the dominant etiological mechanism is neurological entrapment [29], whereas others suggest that vascular occlusion is dominant [30].

MR imaging of the quadrilateral space itself is best demonstrated on oblique coronal views. However, the axillary neurovascular bundle is well visualized on routine oblique sagittal, oblique coronal, and axial images of the shoulder. The nerve should be surrounded by normal fat, without focal enlargement or a mass (Fig. 5). In subacute or chronic denervation of the axillary nerve, edema or atrophy of the teres minor and/or deltoid muscle may be seen. The denervation change of the teres minor muscle is best visualized on the oblique sagittal image [2].

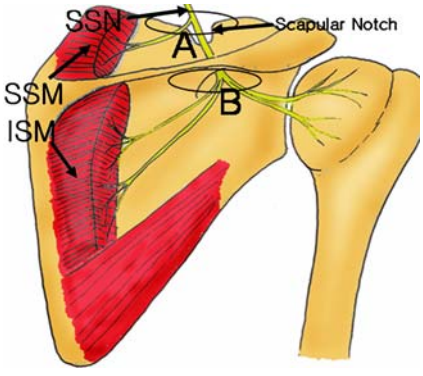

Fig. 3 Schematic diagram of the suprascapular nerve. The suprascapular nerve (*SSN*) traverses the scapular notch beneath the transverse ligament (not shown). The branch to the supraspinatus muscle (*SSM*) leaves just after the SSN passes the scapular notch. The branches to the infraspinatus muscle (*ISM*) fork off after it enters the infraspinatus fossa. If the SSN is compressed around the scapular notch (*A*), both the SSM and ISM would be denervated. If the SSN is compressed around the spinoglenoid notch (*B*), only the ISM would be denervated

Median nerve

Entrapment of the median nerve occurs most commonly in the wrist as carpal tunnel syndrome, but it may also develop at the level of the distal humerus or the proximal end of the forearm [31, 32].

Pronator syndrome

Pronator syndrome is the most proximal entrapment neuropathy of the median nerve [33]. In the region of the elbow, the median nerve passes beneath the bicipital aponeurosis superficial to the brachialis muscle. It then passes between two heads (humeral and ulnar heads) of the pronator teres muscle in approximately 80% of individuals, although the course of the median nerve with respect to the pronator teres can vary. It subsequently passes beneath the edge of the fibrous arch of the flexor digitorum sublimes. The median nerve can be compressed anywhere in these three regions [33] (Fig. 6). Another potential site of compression of the median nerve in the region of the elbow is the ligament of Struthers, which typically connects the supracondylar process to the medial epicondyle. The supracondylar process is usually an incidental finding and occurs in approximately 1% of the population. It is a beak-like bony projection arising from the anteromedial surface of the humerus and is located about 5 cm above the medial epicondyle [34]. Possible causes of pronator syndrome include a fibrous band of the bicipital aponeurosis or hypertrophy of the pronator teres muscle, com-

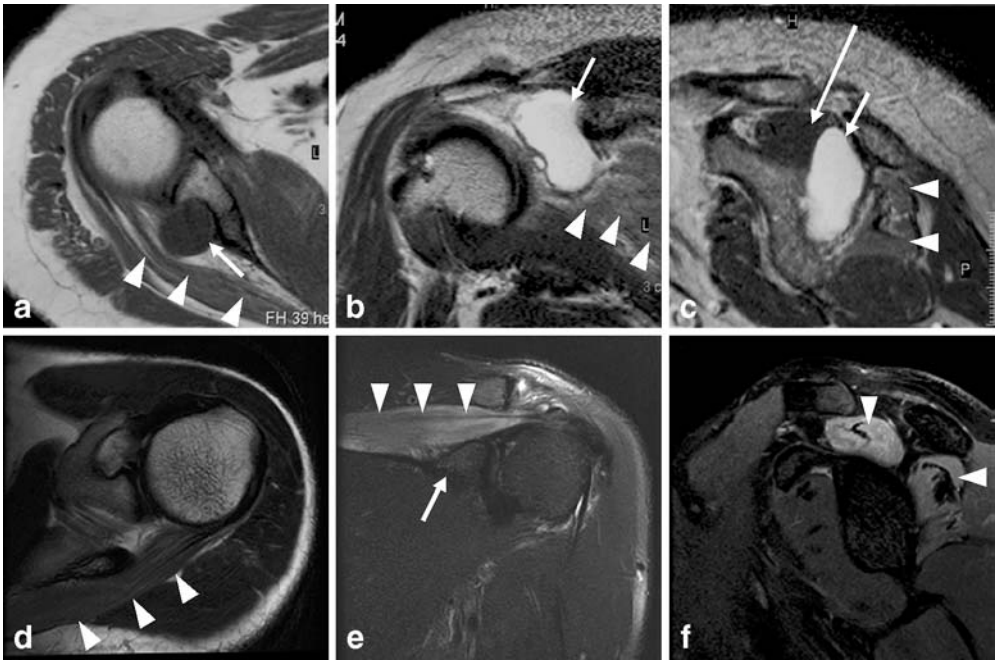

Fig. 4 Entrapment and compression of the suprascapular nerve. **a–c** A cystic lesion (*arrows*) at the spinoglenoid notch is detected on axial T1-weighted image (T1WI) (**a**), coronal fast spin-echo T2-weighted image (FSE T2WI) (**b**), and sagittal FSE T2WI (**c**). Edematous change and slight atrophy of the infraspinatus muscle are attributed to denervation atrophy (*arrowheads*), while the supraspinatus muscle appears normal without atrophy or change in signal intensity (*long arrow* in **c**). These findings suggest that the suprascapular nerve (*SSN*) is compressed around the spinoglenoid notch, even though the nerve is not delineated. **d–f** Axial T1WI (**d**), coronal fat-saturated FSE T2WI (**e**), and sagittal fat-saturated FSE T2WI (**f**) show changes of signal intensity in the supraspinatus and infraspinatus muscles (*arrowheads*)

pression by an aberrant median artery, a crossing branch of the radial artery and vein, hematoma due to trauma, and a soft tissue mass [33, 35]. Patients who have pronator syndrome usually experience a vague, aching pain in the volar aspect of the elbow and forearm, beginning or worsening during activities involving repetitive grasping or pronation or both [33], and sometimes motor disturbances of the first three fingers and sensory abnormalities of the palm of the hand, mimicking carpal tunnel syndrome [36].

Anterior interosseous nerve syndrome (Kiloh–Nevin syndrome)

The anterior interosseous nerve is a purely motor nerve and is the largest branch of the median nerve. It arises on the radial aspect of the median nerve 5 cm to 8 cm distal to the medial epicondyle of the humerus. It passes through the pronator teres and then follows the anterior aspect of the interosseous membrane with the anterior interosseous artery. It provides motor innervation to the flexor pollicis longus (FPL), the radial belly of the flexor digitorum profundus (FDP), and the pronator quadratus (PQ) muscles. Compression and paralysis of this nerve result in a weakness of pinching, although the weakness of pronation may be masked by the concurrent action of the pronator teres [32, 37–39]. There are many causes of anterior interosseous nerve palsy: fracture of the forearm or supracondylar fracture [40, 41], local pressure after sleeping on the affected arm or due to a poorly applied cast, exercise and weight lifting, and viral neuritis [37–39]. In a report of MRI features of anterior interosseous nerve syndrome in three cases [42], an abnormally increased signal intensity of FPL, FDP, and PQ muscles on fast short-tau inversion recovery (STIR) images was noted. The normal anterior interosseous nerve itself cannot be readily identified by MR imaging, so identification of signal intensity changes of innervated muscles is helpful in the diagnosis (Fig. 7).

Carpal tunnel syndrome

The carpal tunnel is a space bordered by the carpal bones and flexor retinaculum (transverse carpal ligament). The space is approximately 6 cm in length from the wrist to the mid-palm. In addition to the median nerve, eight tendons of flexor digitorum profundus and flexor digitorum superficialis (sublimes) and one flexor pollicis longus tendon pass through this space. The flexor retinaculum is approximately 3 cm to 4 cm wide and 2.5 cm to 3.5 mm in thickness. It is attached to the tuberosity of the scaphoid and the crest of the trapezium on the radial side and to the pisiform and the hook of hamate on the ulnar side. On its

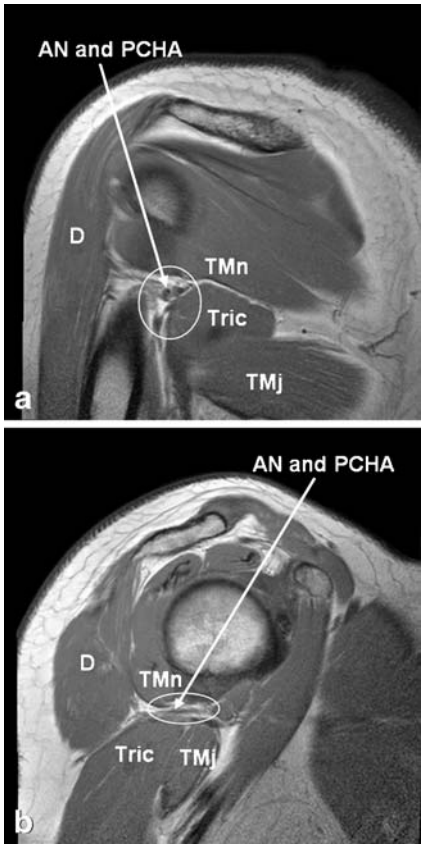

Fig. 5 MR images of the normal quadrilateral space. Oblique coronal proton density-weighted (**a**) and oblique sagittal proton density-weighted (**b**) MR images are well depicting the neurovascular bundle of axillary nerve and posterior circumflex humeral artery within the quadrilateral space (*white lined circles* of **a** and **b**). Note the muscles surrounding the space. Deltoid muscle (*D*) and/or teres minor muscle (*TMn*) are usually denervated in quadrilateral space syndrome. *AN* axillary nerve, *PCHA* posterior circumflex humeral artery, *TMj* teres major muscle, *Tric* long head of triceps muscle

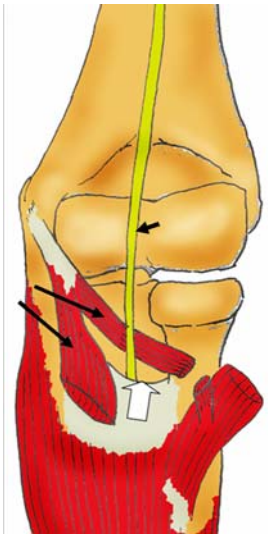

Fig. 6 Schematic diagram of the median nerve at the cubital fossa. The median nerve (*short arrow*) enters the elbow beneath the bicipital aponeurosis (not shown) and then passes between the two heads of the pronator teres muscle (*long arrows*). It subsequently passes beneath the edge of the fibrous arch of the flexor digitorum sublimes (*blank arrow*). These three locations are the potential sites of entrapment

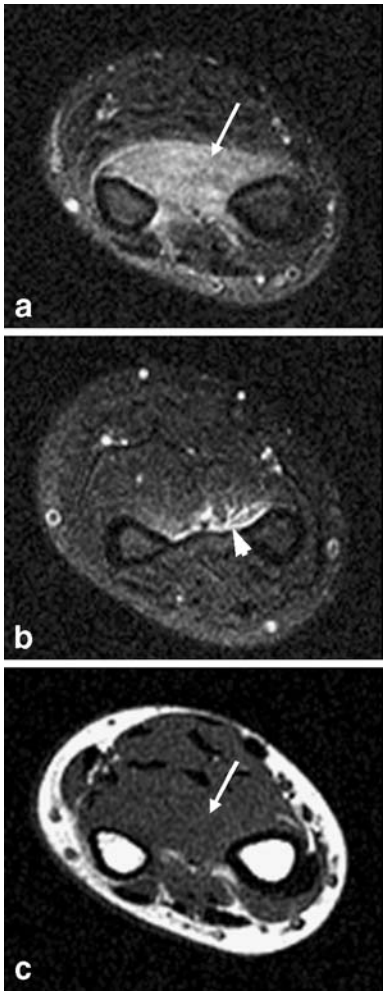

Fig. 7 MR imaging of anterior interosseous nerve syndrome (**a**–**c**). **a**, **c**) At the distal forearm, axial fat-saturated fast spin-echo T2-weighted image (FSE T2WI) (**a**) demonstrates increased signal intensity of the pronator quadratus muscle (*arrows*), whereas a T1-weighted image (T1WI) (**c**) shows no signal change in the muscle. **b** Axial fat-saturated FSE T2WI just proximal to the pronator quadratus muscle shows increased signal intensity anterior to the interosseous membrane where the anterior interosseous neurovascular bundle courses (*arrowhead*). All these findings suggest that there is the possibility of nerve entrapment at this level. Other flexor muscles, such as the flexor pollicis longus and flexor digitorum profundus, do not show signal change

radial side, the flexor retinaculum splits into two layers to envelop the flexor carpi radialis tendon (Fig. 8). The median nerve courses superficial to the flexor digitorum superficialis (FDS) muscle proximal to the carpal tunnel and parallel to the second and third FDS tendons within the carpal tunnel [43]. In the palm, it gives off five branches. The radial branch is the motor nerve innervating the thenar muscles, and the remaining four branches are sensory branches of the first, second, third, and the radial half of the fourth digit [44].

Compression of the median nerve at the carpal tunnel is the most common peripheral nerve entrapment syndrome,

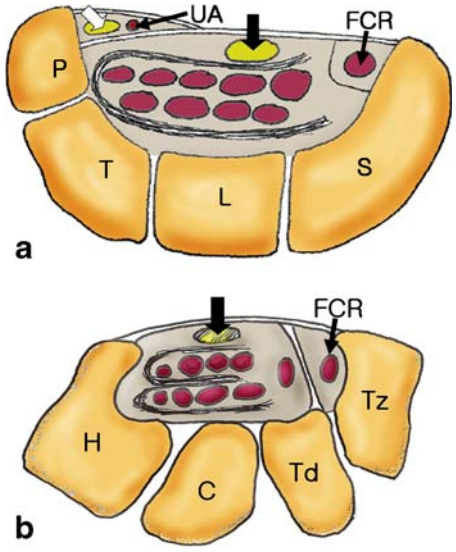

Fig. 8 Schematic diagrams of the carpal tunnel and Guyon's canal at the pisiform level (**a**) and hamate level (**b**). The median nerve (*black arrows*) is passing through the carpal tunnel and is seen volar to the tendons of the second and third FDS. The ulnar nerve (*white arrow*) and ulnar artery (*UA*) pass superficial to the flexor retinaculum on the radial side of the pisiform within Guyon's canal covered by the volar carpal ligament. The flexor carpi radialis tendon (*FCR*) passes between the split fibers of the flexor retinaculum. *P* pisiform, *T* triquetrum, *L* lunate, *S* scaphoid, *H* hamate, *C* capitate, *Td* trapezoid, *Tz* trapezium

with an annual incidence of 50 to 150 cases/100,000 [45]. When the carpal tunnel is narrowed or full of redundant tissue, ischemic changes and subsequent perineurial and epineurial edema of the median nerve develop, resulting in disorders of the axon and nerve sheath. When ischemia lasts for an extended time, irreversible fibrosis of the median nerve develops [43]. Although MR imaging is not always used for routine diagnosis of carpal tunnel syndrome, it can play a role when space-occupying tissue is suspected or in patients with persistent symptoms after carpal tunnel release [46]. Many MR imaging reports have led to the establishment of the golden rule for the exclusive diagnosis of carpal tunnel syndrome, in which four criteria are considered. First, increased signal intensity of the median nerve on a fluid-sensitive sequence is believed to be a sign of carpal tunnel syndrome, although a high signal intensity on STIR imaging is a normal finding, and the signal of the median nerve can be low when the symptom is chronic [2]. Second, an increased size of the median nerve is considered a sign of carpal tunnel syndrome. The normal median nerve is flat at the level of the pisiform. Hence, enlargement of the median nerve is evaluated within the carpal tunnel at the level of the pisiform. Third, volar bowing of the flexor retinaculum at the level of the hamate is believed to demonstrate increased pressure in the carpal tunnel. Fourth, flattening of the median nerve at the level of the hamate is also considered a positive finding. The average cross-sectional area of the median nerve is reported to be 10 mm^2 to 11 mm^2 [47–52] on MR imaging (Fig. 9). These four MR findings are now widely accepted, although they can be nonspecific and observed in asymptomatic individuals [53]. There are various causes of carpal tunnel syndrome, including rheumatoid arthritis, gout, calcium pyrophosphate deposition, acromegaly, hypothyroidism, amyloidosis, neoplasm, ganglion, thrombosis of the median artery, fibrosis of tendons, skeletal anomaly, hemorrhage, and trauma; however, in many cases, the exact etiology remains unidentified [54]. MR imaging can help to identify the causes of carpal tunnel syndrome (Fig. 9). Release of flexor retinaculum is now being performed in cases that remain unresponsive despite conservative treatment.

Ulnar nerve

The ulnar nerve may be involved anywhere along its course in the upper extremity. A patient may have dual pathological abnormalities along the course of the ulnar nerve, a condition referred to as double-crush phenomenon, and may also have an aberrant pathway such as Martin–Gruber anastomosis, which is a median–ulnar nerve connection in the forearm, sometimes resulting in unusual innervation of the hand muscles [55]. Hence, lesion identification in ulnar neuropathy can be very difficult clinically and electrodiagnostically. MR imaging is fundamentally important in the detection of the region of entrapment of the ulnar nerve, although the median and radial nerves can also demonstrate the same diagnostic dilemma [56].

Cubital tunnel syndrome

Ulnar nerve entrapment at the elbow is the second most common entrapment neuropathy [56]. The ulnar nerve passes between the medial epicondyle of the humerus and the olecranon at the condylar groove, deep to the cubital tunnel retinaculum (CTR) and aponeurosis formed between the two heads of the flexor carpi ulnaris (FCU). The CTR and aponeurosis of the flexor carpi ulnaris usually blend with each other, although there are many variations of their blend [57]. The ulnar nerve can be entrapped beneath or near the CTR, and this is called cubital tunnel syndrome [57–59] (Fig. 10). The position of the ulnar nerve in the cubital tunnel changes with the anatomical positioning of the elbow. When the elbow joint is flexed, the ulnar nerve is susceptible to entrapment between the CTR and medial epicondyle of the humerus or it can be dislocated beyond the margin of the CTR; however, the overt symptoms may not always be attributed to the position of the ulnar nerve [57, 60].

Clinical symptoms include a sensory abnormality of the lateral hand and weakness of the flexor carpi ulnaris, flexor digitorum, and intrinsic muscles of the 4th and 5th fingers. Causes of cubital tunnel syndrome include tardy ulnar

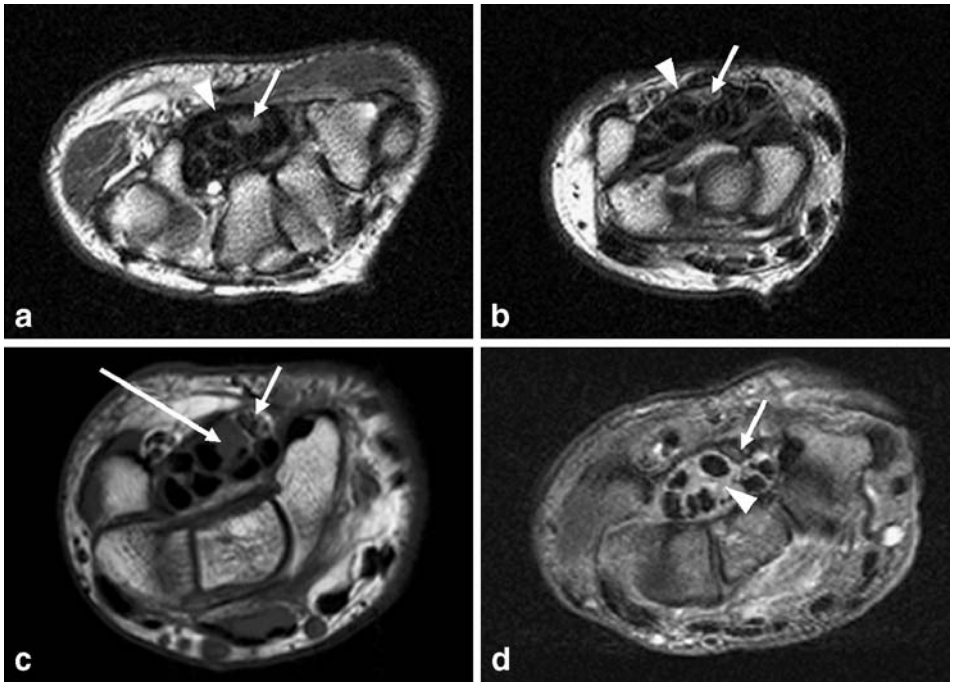

Fig. 9 Various MR imaging features of carpal tunnel syndrome. **a**, **b** Carpal tunnel syndrome without specific causes. Axial fast spin-echo T2-weighted images (FSE T2WIs) at the hamate (**a**) and pisiform (**b**) levels show consistent findings of bowing and thickening of the flexor retinaculum (*arrowhead*). However, the median nerve (*arrow*) itself is flattened and equivocally enlarged, but its signal is increased, which is considered abnormal. **c** Carpal tunnel syndrome caused by anomalous muscle. Axial T1-weighted image (T1WI) of the carpal tunnel at the pisiform level demonstrates anomalous muscle belly of the third flexor digitorum superficialis muscle within the carpal tunnel (*long arrow*). The median nerve (*arrow*) is displaced far radially in the carpal tunnel by this muscle belly. **d** Carpal tunnel syndrome caused by rheumatoid arthritis. Axial fat-saturated FSE T2WI shows tenosynovitis of the flexor digitorum tendons where high signal intensity lesions fill the carpal tunnel (*arrowhead*) and compress the median nerve (*arrow*)

nerve palsy (compression or tension neuropathy of the ulnar nerve at the cubital tunnel due to valgus deformity after trauma), ganglion, accessory epitrochleo-anconeus muscle, subluxation and dislocation of the ulnar nerve.

MR imaging findings of the nerve in cubital tunnel syndrome are enlargement and hyperintense signal around the cubital tunnel compared with a normal segment [56] (Fig. 10).

Guyon's canal syndrome

The ulnar nerve at the wrist passes through a fibro-osseous tunnel known as Guyon's canal. The tunnel extends from the volar carpal ligament at the proximal edge of the pisiform to the origin of the hypothenar muscles at the level of the hamulus, having a distance of approximately 4 cm [61]. The floor of this tunnel is composed of the pisiform, hamate, flexor retinaculum, and hypothenar muscle, and the roof is composed of the volar carpal ligament, palmaris brevis muscle, and fibers of the palmar fascia [62]. The ulnar artery, ulnar nerve, and, occasionally, communicating veins, traverse this space, which is surrounded by fat (Fig. 11). The ulnar nerve enters this space after branching off of the dorsal cutaneous branch and divides into the superficial sensory nerve and the deep motor nerve within this space [62]. The motor nerve branch innervates the palmaris brevis, hypothenar muscle, lateral lumbrical and interosseous muscle, adductor pollicis, and abductor digiti minimi muscles. The clinical importance of this tunnel is that it may become the site of ulnar nerve compression. The causes of such compression include: space-occupying lesions, such as ganglion, lipoma, uremic tumoral calcinosis, trauma, and anatomic muscular variants, such as abductor digiti minimi coursing through this canal [63–65]. Vascular abnormalities, such as aneurysm and thrombosis of the ulnar artery due to repeated trauma (e.g., bicycle riding, judo, tennis), can result in an ulnar nerve abnormality called "hypothenar hammer syndrome" [66].

When a dedicated wrist coil is used, MR imaging offers a reliable means of evaluating Guyon's canal. The average diameter of the ulnar nerve at the pisiform level on MR imaging is 3 mm, and bifurcation occurs an average of 12 mm beyond the tunnel inlet. The deep motor branch is quickly obscured by adjacent muscle after its bifurcation [67]. The usefulness of MR imaging in Guyon's canal syndrome is in the detection of space-occupying lesions within the canal and/or signal intensity and size changes of the nerve itself (Fig. 11).

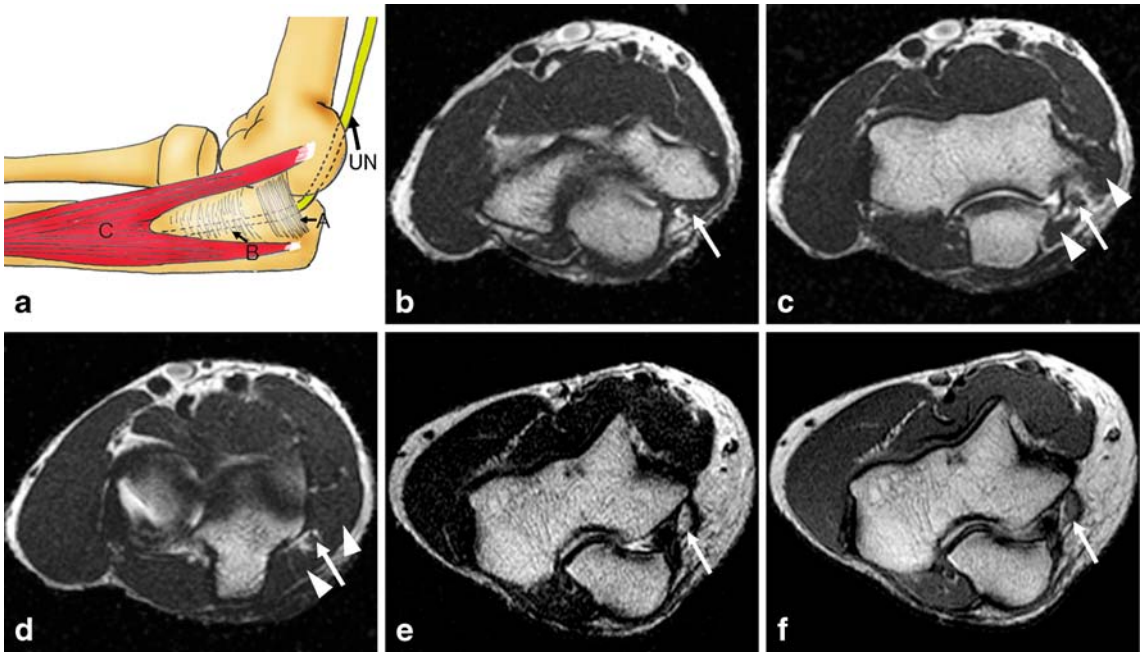

Fig. 10 Schematic diagram of the cubital tunnel and MR imaging features of a normal and an entrapped ulnar nerve around the cubital tunnel. **a** Schematic diagram of the cubital tunnel shows that the ulnar nerve enters the cubital tunnel beneath the CTR (*A*), subsequently passing deep to the aponeurosis (**b**), which is formed between the two heads of the FCU muscle (**c**). **b–d** Axial T1-weighted images (T1WIs) of the normal cubital tunnel from the proximal (**b**) to the distal (**d**) levels. Note the location and size of the normal ulnar nerve (*arrows*) in the cubital tunnel. The two heads of the FCU are shown (*arrowheads*). **e**, **f** Axial fast spin-echo T2-weighted image (FSE T2WI) (**e**) and a proton density-weighted image (**f**) of entrapped neuropathy of the ulnar nerve at the level of the proximal cubital tunnel. The ulnar nerve (*arrows*) is certainly enlarged in comparison with the ulnar nerve more proximal or distal to the cubital tunnel (not shown)

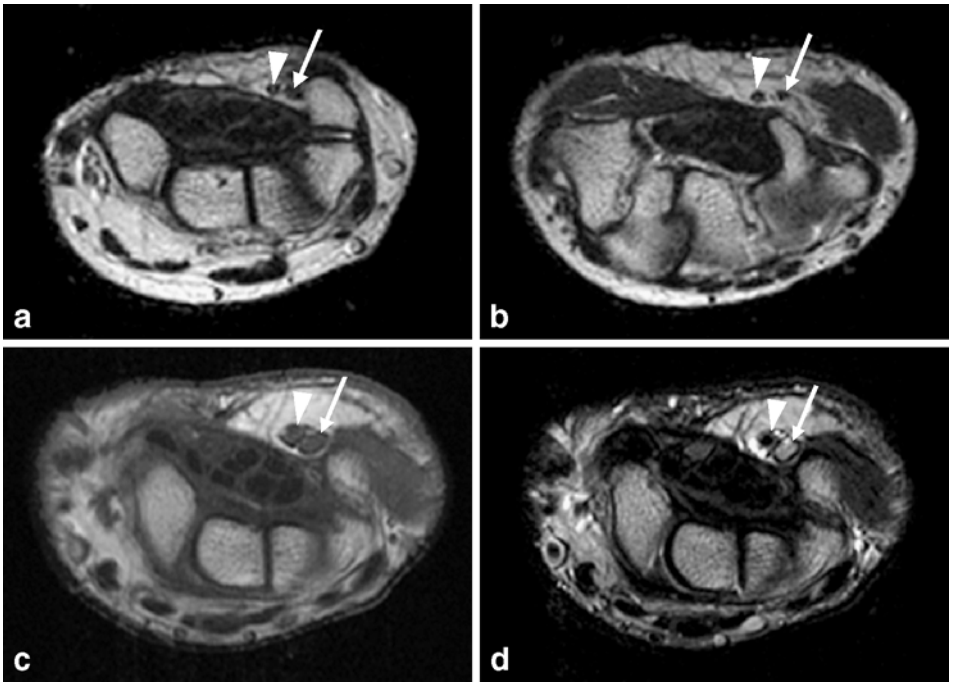

Fig. 11 MR imaging features of normal and entrapped ulnar nerves within Guyon's canal. **a**, **b** Axial T1-weighted images (T1WIs) of Guyon's canal at the level of the pisiform (**a**) and hamate (**b**). The ulnar nerve (*arrows*) is seen within Guyon's canal, passing radial to the pisiform and volar to the hamate. Note that the ulnar artery (*arrowheads*) passes more radially. **c**, **d** Axial T1WI (**c**) and fast spin-echo T2-weighted image (FSE T2WI) of a patient suffering from numbness of the hand on the ulnar side. The ulnar nerve (*arrows*) is increased in size and signal intensity (**d**). *Relatively prominent fat surrounding ulnar nerve and artery within the Guyon's canal ,which was confirmed to be the lipoma on surgery, is seen.* Note the location of the ulnar artery again (*arrowheads*)

Radial nerve

Saturday night palsy and other radial nerve palsies of the upper arm

The radial nerve is the largest branch of the brachial plexus and is the main continuation of its posterior cord. It passes between the long and medial and subsequently between the medial and lateral heads of the triceps muscle, posterior to the humeral diaphysis (spiral groove of the humerus) at the mid-diaphysis of the humerus. The spiral groove is prone to entrapment of the radial nerve, particularly when people sleep with their arms held in an improper position [68, 69]. Consequently, weakness of the triceps, brachioradialis, and extensor and supinator muscles of the hand and wrist develops.

The radial nerve is also often injured when a humeral shaft fracture occurs at the middle and distal thirds of the humerus, owing to the close anatomic relationship of the radial nerve with the bone as the nerve courses through the middle and distal thirds of the upper arm and because of the diminished mobility of the nerve where it pierces the lateral muscular septum. MR imaging can depict the radial nerve in these locations along the humeral shaft, but inherent limited spatial resolution of MR imaging often makes reliable depiction of it difficult. A previous report represented the ultrasound (US) morphologies of the normal and injured radial nerves by humeral shaft fracture. Surgically proven morphologies of traumatized nerves by humeral shaft fracture, in the report, were as follows: thinned and pinched between dislocated bone fragment; complete disruption of the nerve with stump neuroma; flattened and stretched over the fixation device for fracture; thickened over the displaced fracture segment; nerve buried in the callus [70].

Radial tunnel syndrome and posterior interosseous nerve syndrome

Compression at the radial tunnel is the most common entrapment neuropathy of the radial nerve. The radial tunnel is an anatomic space of the elbow that is approximately 5 cm in length, extending from the capit-

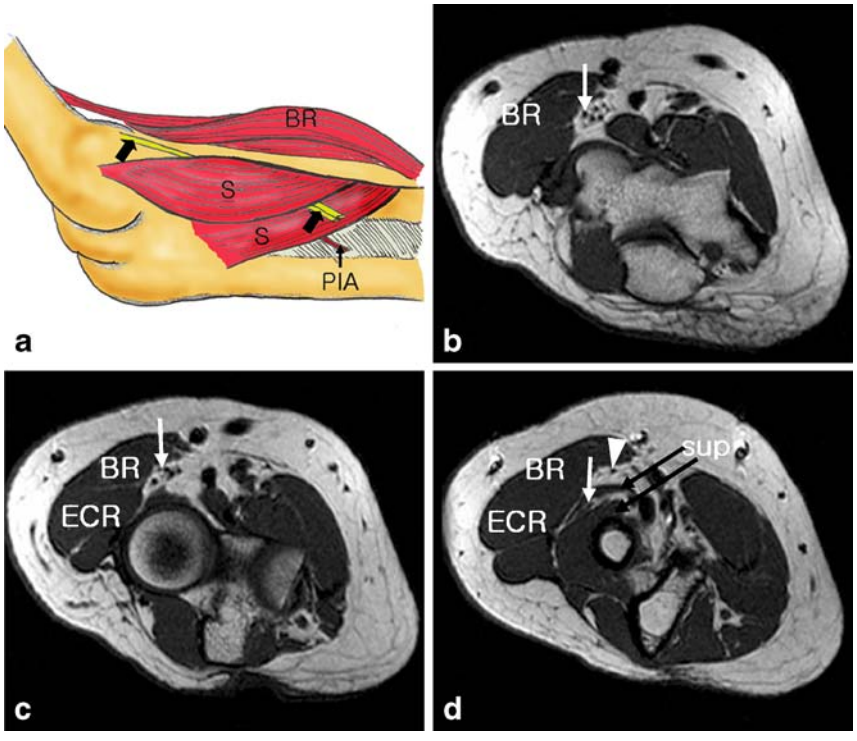

Fig. 12 Schematic diagram and MR imaging of the normal radial nerve at the level of the elbow. **a** Schematic diagram of the course of the posterior interosseous nerve. The radial nerve passes deep to the brachioradialis muscle (*BR*) and branches into the superficial branch and deep branch (posterior interosseous nerve, *arrows*). The superficial branch (not shown) passes superficial to the supinator muscle. The deep branch courses between the deep and superficial heads of the supinator muscle (*S*) and can be compressed by the arcade of Frohse, which is a fibrous band at the origin of the supinator muscle. **b–d** Three consecutive axial T1-weighted images (T1WIs) of the elbow visualizing the normal course of the radial nerve. Note the radial neurovascular bundle as clustered dots (*arrows* in **b** and **c**). It passes deep to the BR and extensor carpi radialis (*ECR*) muscles. The superficial branch passes deep to the brachioradialis and superficial to the supinator muscle (*arrowhead* in **d**). The deep branch (posterior interosseous nerve *arrow* in **d**) passes between the two heads of the supinator muscle (*sup*) forming the posterior interosseous nerve, which innervates the extensor muscles of the forearm. *PIA* posterior interosseous artery

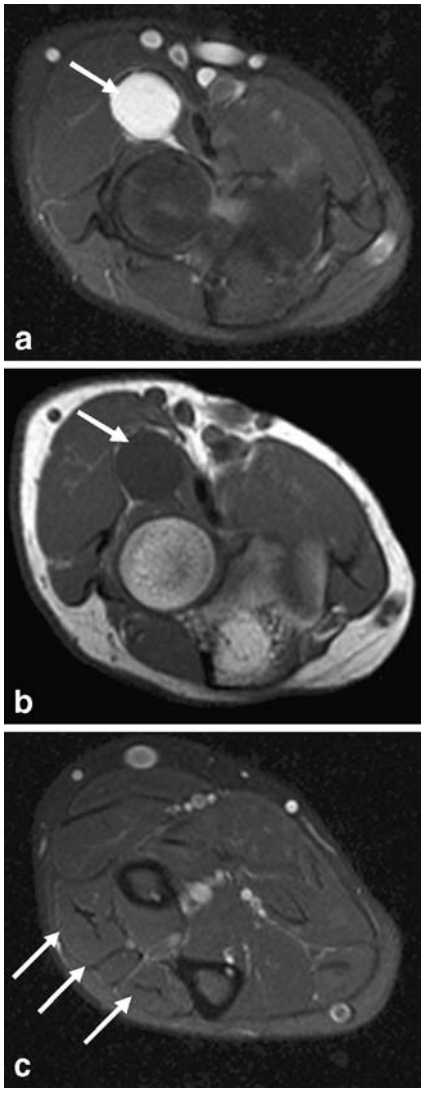

Fig. 13 MR imaging of a patient with radial nerve compressive neuropathy presenting with dorsoradial numbness of the forearm. **a**, **b** Axial fat-saturated fast spin-echo T2-weighted image (FSE T2WI) (**a**) and T1-weighted image (T1WI) (**b**) at the level of the radial head demonstrate a cystic lesion (*arrows*), which can compress nearby radial nerves. However, axial fat-saturated FSE T2WI at the level of the proximal forearm (**c**) does not show denervation change of the extensor muscles (*arrows*). No motor weakness of the extensor muscles is present

ulum of the humerus to the distal edge of the supinator muscle, through which the radial nerve traverses. The radial tunnel is bounded posteriorly by the capitulum, anteromedially by the brachialis muscle, and anterolaterally by the brachioradialis and extensor carpi radialis brevis muscles. The radial nerve divides into the superficial branch and the deep branch (called the posterior interosseous nerve) at a level distal to the lateral epicondyle of the humerus and proximal to the supinator muscle [71]. The superficial branch passes superficial to the supinator muscle and continues to the lateral forearm, providing only sensory branches to the dorsoradial hand. In contrast, the posterior interosseous nerve passes in a plane between the deep and superficial heads of the supinator muscle, where the nerve can be compressed by the arcade of Frohse. The posterior interosseous nerve continues into the forearm, traveling deep along the extensor surface of the interosseous membrane, branching off the motor fibers to the extensor muscles of the forearm (Fig. 12).

Potential sites of nerve compression within the radial tunnel are the fibrous band anterior to the radial head that

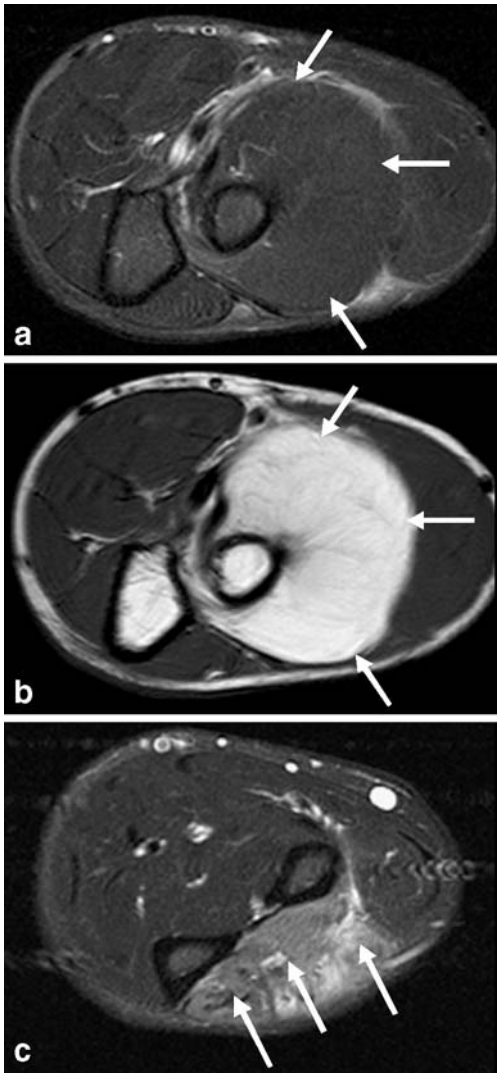

Fig. 14 MR imaging features of posterior interosseous nerve syndrome. **a**, **b** Axial fat-saturated fast spin-echo T2-weighted image (FSE T2WI) (**a**) and T1-weighted image (T1WI) (**b**) at the proximal forearm demonstrate a huge lipoma (*arrows*) between the radius and supinator muscle, possibly compressing the posterior interosseous nerve branching off from the radial nerve. **c** Axial fat-saturated FSE T2WI at the mid-forearm shows increased signal intensity and mild atrophy of the extensor muscles (*arrows*),

anchors the radial nerve or its branches to the elbow joint; the tendinous edge of extensor carpi radialis brevis; the vessel group of the radial recurrent artery and its branches, which is called the leash of Henry; the arcade of Frohse, a fibrous band at the origin of the supinator muscle; and the fascial arcade at the distal end and lateral side of the supinator muscle [71–74].Although the terms *radial tunnel syndrome* and *posterior interosseous nerve syndrome* are somewhat confusing and occasionally coincide, owing to their similar causes and anatomic location, they are distinguished on the basis of different clinical presentations. Radial tunnel syndrome presents primarily with pain and occasional sensory disturbances, without significant weakness. Posterior interosseous nerve syndrome, on the other hand, presents primarily with motor weakness of the extensor muscle group, which is called 'wrist drop'. This syndrome is not accompanied by significant sensory loss [71].

Nerve entrapment at the radial tunnel may result from direct compression at anatomic sites mentioned previously. Dynamic compression may also be caused by repetitive pronation and supination, such as that experienced by violinists, music conductors, and swimmers [71]. Mechanical compression can be attributed to the ganglion cyst (Fig. 13), lipoma (Fig. 14), vascular malformation, synovitis, bicipitoradial bursitis, swelling from trauma, and radial head dislocation [2]. MR imaging can disclose the causes of mechanical compression.

Conclusion

For the evaluation of NECS, both MR imaging and ultrasound provide excellent direct visualization of the nerve and surrounding abnormalities such as space-occupying lesions. Hence, these imaging modalities can play a cooperative role with electrodiagnostic studies in diagnosing NECS in atypical or inconclusive cases.

Although ultrasound is widely used for nerve imaging, the inherent drawback of operator dependency makes MR imaging an imaging tool of choice for entrapment and compressive neuropathies. Moreover, in the era of high-generation MR equipment, higher spatial resolution of MR imaging is expected to realize more convincing visualization of the nerves.

In conclusion, we believe that it is critical for radiologists to be familiar with the normal morphology and anatomy of nerve passages on MR imaging, the muscular innervations of the affected nerve, and MR imaging features of entrapment and compressive neuropathies.

References

1. Spratt JD, Stanley AJ, Grainger AJ, Hide IG, Campbell RS (2002) The role of diagnostic radiology in compressive and entrapment neuropathies. Eur Radiol 12:2352–2364
2. Hochman MG, Zilberfarb JL (2004) Nerves in a pinch: imaging of nerve compression syndromes. Radiol Clin North Am 42:221–245
3. Bacigalupo L, Bianchi S, Valle M, Martinoli C (2003) Ultrasonography of peripheral nerves. Radiologe 43:841–849
4. Beekman R, Visser LH (2004) High-resolution sonography of the peripheral nervous system—a review of the literature. Eur J Neurol 11:305–314
5. Chiou HJ, Chou YH, Chiou SY, Liu JB, Chang CY (2003) Peripheral nerve lesions: role of high-resolution US. Radiographics 23:e15
6. Grant GA, Britz GW, Goodkin R, Jarvik JG, Maravilla K, Kliot M (2002) The utility of magnetic resonance imaging in evaluating peripheral nerve disorders. Muscle Nerve 25:314–331
7. Howe FA, Filler AG, Bell BA, Griffiths JR (1992) Magnetic resonance neurography. Magn Reson Med 28:328–338
8. Kuntz Ct, Blake L, Britz G, Filler A, Hayes CE, Goodkin R, Tsuruda J, Maravilla K, Kliot M (1996) Magnetic resonance neurography of peripheral nerve lesions in the lower extremity. Neurosurgery 39:750–756; discussion 756–757
9. Lee CH, Kim TK, Yoon ES, Dhong ES (2005) Correlation of high-resolution ultrasonographic findings with the clinical symptoms and electrodiagnostic data in carpal tunnel syndrome. Ann Plast Surg 54:20–23
10. Martinoli C, Bianchi S, Gandolfo N, Valle M, Simonetti S, Derchi LE (2000) US of nerve entrapments in osteofibrous tunnels of the upper and lower limbs. Radiographics 20:S199–S217
11. Stuart RM, Koh ES, Breidahl WH (2004) Sonography of peripheral nerve pathology. AJR Am J Roentgenol 182:123–129
12. Atasoy E (2004) Thoracic outlet syndrome: anatomy. Hand Clin 20:7–14;
13. Bowen BC, Pattany PM, Saraf-Lavi E, Maravilla KR (2004) The brachial plexus: normal anatomy, pathology, and MR imaging. Neuroimaging Clin N Am 14:59–85; vii–viii
14. Demondion X, Bacqueville E, Paul C, Duquesnoy B, Hachulla E, Cotten A (2003) Thoracic outlet: assessment with MR imaging in asymptomatic and symptomatic populations. Radiology 227:461–468
15. Blair DN, Rapoport S, Sostman HD, Blair OC (1987) Normal brachial plexus: MR imaging. Radiology 165:763–767
16. Panegyres PK, Moore N, Gibson R, Rushworth G, Donaghy M (1993) Thoracic outlet syndromes and magnetic resonance imaging. Brain 116:823–841
17. Smedby O, Rostad H, Klaastad O, Lilleas F, Tillung T, Fosse E (2000) Functional imaging of the thoracic outlet syndrome in an open MR scanner. Eur Radiol 10:597–600
18. Fritz RC, Helms CA, Steinbach LS, Genant HK (1992) Suprascapular nerve entrapment: evaluation with MR imaging. Radiology 182:437–444
19. Post M, Grinblat E (1992) Nerve entrapment about the shoulder girdle. Hand Clin 8:299–306

20. Sallomi D, Janzen DL, Munk PL, Connell DG, Tirman PF (1998) Muscle denervation patterns in upper limb nerve injuries: MR imaging findings and anatomic basis. AJR Am J Roentgenol 171:779–784
21. Rengachary SS, Burr D, Lucas S, Brackett CE (1979) Suprascapular entrapment neuropathy: a clinical, anatomical, and comparative study. Part 3: comparative study. Neurosurgery 5:452–455
22. Zehetgruber H, Noske H, Lang T, Wurnig C (2002) Suprascapular nerve entrapment. A meta-analysis. Int Orthop 26:339–343
23. Takagishi K, Maeda K, Ikeda T, Itoman M, Yamamoto M (1991) Ganglion causing paralysis of the suprascapular nerve. Diagnosis by MRI and ultrasonography. Acta Orthop Scand 62:391–393
24. Elsayes KM, Shariff A, Staveteig PT, Mukundan G, Khosla A, Rubin DA (2005) Value of magnetic resonance imaging for muscle denervation syndromes of the shoulder girdle. J Comput Assist Tomogr 29:326–329
25. Cahill BR, Palmer RE (1983) Quadrilateral space syndrome. J Hand Surg [Am] 8:65–69
26. Chautems RC, Glauser T, Waeber-Fey MC, Rostan O, Barraud GE (2000) Quadrilateral space syndrome: case report and review of the literature. Ann Vasc Surg 14:673–676
27. Hoskins WT, Pollard HP, McDonald AJ (2005) Quadrilateral space syndrome: a case study and review of the literature. Br J Sports Med 39:e9
28. Robinson P, White LM, Lax M, Salonen D, Bell RS (2000) Quadrilateral space syndrome caused by glenoid labral cyst. AJR Am J Roentgenol 175:1103–1105
29. Lester B, Jeong GK, Weiland AJ, Wickiewicz TL (1999) Quadrilateral space syndrome: diagnosis, pathology, and treatment. Am J Orthop 28:718–722; 725
30. Dugas JR, Weiland AJ (2000) Vascular pathology in the throwing athlete. Hand Clin 16:477–485; x
31. Morgan RF, Terranova W, Nichter LS, Edgerton MT (1985) Entrapment neuropathies of the upper extremity. Am Fam Physician 31:123–134
32. Wertsch JJ, Melvin J (1982) Median nerve anatomy and entrapment syndromes: a review. Arch Phys Med Rehabil 63:623–627
33. Rehak DC (2001) Pronator syndrome. Clin Sports Med 20:531–540
34. Lordan J, Rauh P, Spinner RJ (2005) The clinical anatomy of the supracondylar spur and the ligament of Struthers. Clin Anat 18:548–551
35. Johnson RK, Spinner M, Shrewsbury MM (1979) Median nerve entrapment syndrome in the proximal forearm. J Hand Surg [Am] 4:48–51
36. Lee MJ, LaStayo PC (2004) Pronator syndrome and other nerve compressions that mimic carpal tunnel syndrome. J Orthop Sports Phys Ther 34:601–609
37. Eversmann WW (1992) Proximal median nerve compression. Hand Clin 8:307–315
38. Schantz K, Riegels-Nielsen P (1992) The anterior interosseous nerve syndrome. J Hand Surg [Br] 17:510–512
39. Seror P (1996) Anterior interosseous nerve lesions. Clinical and electrophysiological features. J Bone Joint Surg Br 78:238–241
40. Joist A, Joosten U, Wetterkamp D, Neuber M, Probst A, Rieger H (1999) Anterior interosseous nerve compression after supracondylar fracture of the humerus: a metaanalysis. J Neurosurg 90:1053–1056
41. Nicholls MA, Lawton JN, Lawrence SJ (2003) Radiologic case study. Radial shaft fracture, anterior interosseous nerve injury, and the presence of a foreign body within the soft tissues of the proximal forearm. Orthopedics 26:111–112
42. Grainger AJ, Campbell RS, Stothard J (1998) Anterior interosseous nerve syndrome: appearance at MR imaging in three cases. Radiology 208:381–384
43. Omer GE Jr (1992) Median nerve compression at the wrist. Hand Clin 8:317–324
44. Shuman S, Osterman L, Bora FW (1987) Compression neuropathies. Semin Neurol 7:76–87
45. Martin BI, Levenson LM, Hollingworth W, Kliot M, Heagerty PJ, Turner JA, Jarvik JG (2005) Randomized clinical trial of surgery versus conservative therapy for carpal tunnel syndrome [ISRCTN84286481]. BMC Musculoskelet Disord 6:2
46. Maurer J, Bleschkowski A, Tempka A, Felix R (2000) High-resolution MR imaging of the carpal tunnel and the wrist. Application of a 5-cm surface coil. Acta Radiol 41:78–83
47. Bordalo-Rodrigues M, Amin P, Rosenberg ZS (2004) MR imaging of common entrapment neuropathies at the wrist. Magn Reson Imaging Clin N Am 12:265–279; vi
48. Jarvik JG, Yuen E, Haynor DR, Bradley CM, Fulton-Kehoe D, Smith-Weller T, Wu R, Kliot M, Kraft G, Wang L, Erlich V, Heagerty PJ, Franklin GM (2002) MR nerve imaging in a prospective cohort of patients with suspected carpal tunnel syndrome. Neurology 58:1597–1602
49. Jarvik JG, Yuen E, Kliot M (2004) Diagnosis of carpal tunnel syndrome: electrodiagnostic and MR imaging evaluation. Neuroimaging Clin N Am 14:93–102; viii
50. Mesgarzadeh M, Schneck CD, Bonakdarpour A, Mitra A, Conaway D (1989) Carpal tunnel: MR imaging. Part II. Carpal tunnel syndrome. Radiology 171:749–754
51. Mesgarzadeh M, Triolo J, Schneck CD (1995) Carpal tunnel syndrome. MR imaging diagnosis. Magn Reson Imaging Clin N Am 3:249–264
52. Monagle K, Dai G, Chu A, Burnham RS, Snyder RE (1999) Quantitative MR imaging of carpal tunnel syndrome. AJR Am J Roentgenol 172:1581–1586
53. Radack DM, Schweitzer ME, Taras J (1997) Carpal tunnel syndrome: are the MR findings a result of population selection bias? AJR Am J Roentgenol 169:1649–1653
54. Lee D, van Holsbeeck MT, Janevski PK, Ganos DL, Ditmars DM, Darian VB (1999) Diagnosis of carpal tunnel syndrome. Ultrasound versus electromyography. Radiol Clin North Am 37:859–872; x
55. Lee KS, Oh CS, Chung IH, Sunwoo IN (2005) An anatomic study of the Martin–Gruber anastomosis: electrodiagnostic implications. Muscle Nerve 31:95–97
56. Britz GW, Haynor DR, Kuntz C, Goodkin R, Gitter A, Maravilla K, Kliot, M (1996) Ulnar nerve entrapment at the elbow: correlation of magnetic resonance imaging, clinical, electrodiagnostic, and intraoperative findings. Neurosurgery 38:458–465; discussion 465
57. O'Driscoll SW, Horii E, Carmichael SW, Morrey BF (1991) The cubital tunnel and ulnar neuropathy. J Bone Joint Surg Br 73:613–617
58. Barrios C, Ganoza C, de Pablos J, Canadell J (1991) Posttraumatic ulnar neuropathy versus non-traumatic cubital tunnel syndrome: clinical features and response to surgery. Acta Neurochir (Wien) 110:44–48

59. Campbell WW, Pridgeon RM, Riaz G, Astruc J, Sahni KS (1991) Variations in anatomy of the ulnar nerve at the cubital tunnel: pitfalls in the diagnosis of ulnar neuropathy at the elbow. Muscle Nerve 14:733–738
60. Rosenberg ZS, Bencardino J, Beltran J (1997) MR imaging of normal variants and interpretation pitfalls of the elbow. Magn Reson Imaging Clin N Am 5:481–499
61. Gross MS, Gelberman RH (1985) The anatomy of the distal ulnar tunnel. Clin Orthop Relat Res:196:238–247
62. Moneim MS (1992) Ulnar nerve compression at the wrist. Ulnar tunnel syndrome. Hand Clin 8:337–344
63. Bui-Mansfield LT, Williamson M, Wheeler DT, Johnstone F (2002) Guyon's canal lipoma causing ulnar neuropathy. AJR Am J Roentgenol 178:1458
64. Garcia S, Cofan F, Combalia A, Campistol JM, Oppenheimer F, Ramon R (2000) Compression of the ulnar nerve in Guyon's canal by uremic tumoral calcinosis. Arch Orthop Trauma Surg 120:228–230
65. Ruocco MJ, Walsh JJ, Jackson JP (1998) MR imaging of ulnar nerve entrapment secondary to an anomalous wrist muscle. Skeletal Radiol 27:218–221
66. Liskutin J, Dorffner R, Resinger M, Silberbauer K, Mostbeck G (2000) Hypothenar hammer syndrome. Eur Radiol 10:542
67. Zeiss J, Jakab E, Khimji T, Imbriglia J (1992) The ulnar tunnel at the wrist (Guyon's canal): normal MR anatomy and variants. AJR Am J Roentgenol 158:1081–1085
68. Bora FW Jr, Osterman AL (1982) Compression neuropathy. Clin Orthop 163:20–32
69. Reddy MP (1983) Peripheral nerve entrapment syndromes. Am Fam Physician 28:133–143
70. Bodner G, Buchberger W, Schocke M, Bale R, Huber B, Harpf C, Gassner E, Jaschke W (2001) Radial nerve palsy associated with humeral shaft fracture: evaluation with US—initial experience. Radiology 219:811–816
71. Kleinert JM, Mehta S (1996) Radial nerve entrapment. Orthop Clin North Am 27:305–315
72. Chien AJ, Jamadar DA, Jacobson JA, Hayes CW, Louis DS (2003) Sonography and MR imaging of posterior interosseous nerve syndrome with surgical correlation. AJR Am J Roentgenol 181:219–221
73. Konjengbam M, Elangbam J (2004) Radial nerve in the radial tunnel: anatomic sites of entrapment neuropathy. Clin Anat 17:21–25
74. Ritts GD, Wood, MB, Linscheid RL (1987). Radial tunnel syndrome. A ten-year surgical experience. Clin Orthop Relat Res 219:201–205